Effects of annealing temperature on properties of SiO_2 nanoparticles for supercapacitor applications

J.Thenmozhi[1], E.Kavitha[2*], N.Sundaraganesan[3]

[1]*Department of Physics, Annmalai University, Annamalainagar-608002, Tamilnadu, India.*

[2]*Department of Physics, NRK Govt Arts College for Women, Namakkal-637001, Tamilnadu, India.*

[3]*Department of Physics, Annmalai University, Annamalainagar-608002, Tamilnadu, India.*

* Corresponding Author

Dr. E.Kavitha

Assistant Professor

Department of Physics,

NRK Govt Arts College for Women,

Namakkal-637001,

Tamilnadu, India.

Cell: +91-8637430882

Abstract

In this work, a sol-gel method for preparing nanosized SiO_2 for supercapacitor applications. Tetraethyl orthosilicate was used as precursor and PVP as surfactant for the synthesis of SiO_2 nanoparticles. The effect of annealing temperature on prepared SiO_2 nanoparticles (NPs) was examined through the thermal, structural, morphological, and electrochemical characteristics. The thermal properties of as-prepared SiO_2 nanoparticles were evaluated using TG-DTA analysis. The X-ray diffraction result suggested that the prepared nanoparticles had amorphous structure and the average crystallite size decreased with increasing annealing temperatures. The SEM micrographs showed the SiO_2 NPs appeared as an aggregated bundle-like structure. The EDX analysis confirmed the existence of elements of Si and O. The

oxidation and reduction peaks revealed that the SiO_2 NPs had a supercapacitor nature by cyclic voltammetry and achieved high specific capacitance value of 356 Fg^{-1} at scan rate of 5 mV/s. These findings suggest that SiO_2 NPs, which offer a cost-effective and scalable approach, are promising candidates for supercapacitor electrodes

Keywords: Supercapacitor, Pseudocapacitor, annealing temperature, SiO_2 NPs.

1. Introduction

The scientific world has focused a great deal of interest on silica nanoparticles because of its numerous uses in drugs, electronics, insulators, and catalysis. The oxide nanoparticles produced using various techniques have well electrical, optical, magnetic, thermal energy storage, solar energy conversion, and as additives in nanofluids they seem to be more beneficial [1-4]. There has been a lot of interest in silica nanoparticles for use in pigments, drugs, catalysis, and medicines [5]. The materials substrates, humidity sensors, electrical insulators, thermal insulators, and electronic substrates are all made with amorphous SiO_2 nanoparticles. Each of these products has a distinct function for the silica particles. Some of these goods quality is significantly influenced by the size and spatial dispersion of the particles of silica [6]. High-purity silica particles with a narrow size distribution are crucial because high-tech industries like biotechnology and photonics are increasing their demand for these materials [7]. Regarding surface defects associated with large surface/volume ratios, Si nanoparticles can be obtained among respect to their structural, functional, morphological and optical characteristics [8]. Silica nanoparticles are prepared by a variety of methods, including as sol-gel processing, combustion synthesis, hydrothermal processes, chemical vapour deposition, micro emulsion

processing, and plasma synthesis [9]. The primary objective was to regulate the size, shape, and surface reactivity of the particles regardless of the synthesis method. The most widely used method for synthesis silica nanoparticles is the sol-gel procedure, which involves the metal alkoxides simultaneous hydrolysis and condensation reaction. Along with numerous techniques, the sol-gel approach offers a few benefits, including low temperature synthesis and chemical composition-based reaction kinetics control [10 - 12]. Mesoporous silica nanospheres that were synthesized using various cationic surfactants and polyvinyl pyrrolidine were reported to have homogeneous size and shape [13]. Many benefits of the sol-gel process over other approaches include its convenience, adaptability, purity, homogeneity, and changes of by altering the synthesis parameters, material qualities [14].

2. Preparation of silicon dioxide (SiO_2) nanoparticles

The sol-gel technique was used to synthesis SiO_2 nanoparticles. There was no need for additional purification because every reagent utilized was analytical grade. In this work, we have used tetraethylorthosilicate (99.9%, Aldrich), absolute ethanol (EtOH 99.5%, Aldrich), Glycolic acid (EMPULRA), and Polyvinylpyrolidone PVP (LOBA). Glycolic acid (2.3 ml) was added to a stirred solution of Tetraethylorthosilicate (TEOS) (2.2 ml), and the stirring was left for ten minutes. To create sol, slowly add 12 ml of a 5 weight percent PVP solution in ethanol was added drop wise to above solution and the mixture was allowed to stir for one hour in order form °he sol. The sol turned into a gel after a full day of ageing. The gel was dried at 100 °C 1 for hour in order to evaporate water and organic compounds. After drying, SiO_2 product was annealed at different temperature (500 °C, 600 °C, 700 °C and 800 °C) and grained to obtain fine white colored nanoparticles. After annealed, the prepared samples were characterized using Thermo gravimetric analysis (TG-DTA), X-Ray diffraction (XRD), Fourier Transform Infrared

Spectroscopy (FT-IR), Scanning electron microscope (SEM-EDX) and Cyclic Voltammetry (CV).

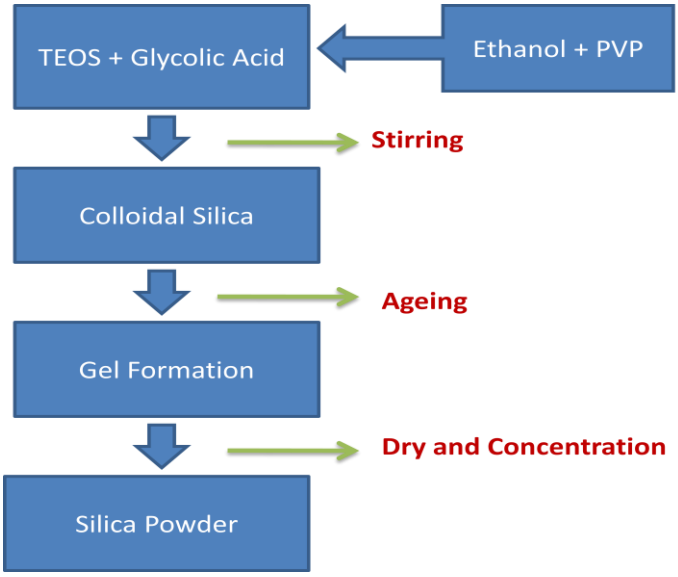

Fig. 1. Synthesis process of SiO_2 nanoparticles.

3. Results and discussion

3.1. Thermal analysis (TG-DTA)

The thermal analysis of as-prepared SiO_2 nanoparticles was studied by TG-DTA analysis. In order to do that, curves were recorded in the nitrogen environment between ambient temperatures to 1000 °C, increasing at a rate of 20 °C per minute. The TG/DTA curve for SiO_2 nanoparticles are shown in Fig. 2. It is evident from the figure, the TG curve showed the three stages of weight loss. The desorption of the sample water content may be the cause of the first weight loss seen below 180 °C. It's possible that the breakdown of organic and inorganic templates leading to the final product's crystallization is the cause of the anticipated final weight loss in the 190 – 390 ^oC range. The final weight loss brought on by the SiO_2 nanoparticles

formation at temperatures between 370 - 480 ºC. An endothermic peak observed at 240 °C is shown in the DTA curve, was corresponded to water content is degrading. On the other hand, the formation of SiO_2 nanoparticles and the thermal breakdown of glycolic acid the cause of the exothermic peak that appears at 535 °C [15-19].

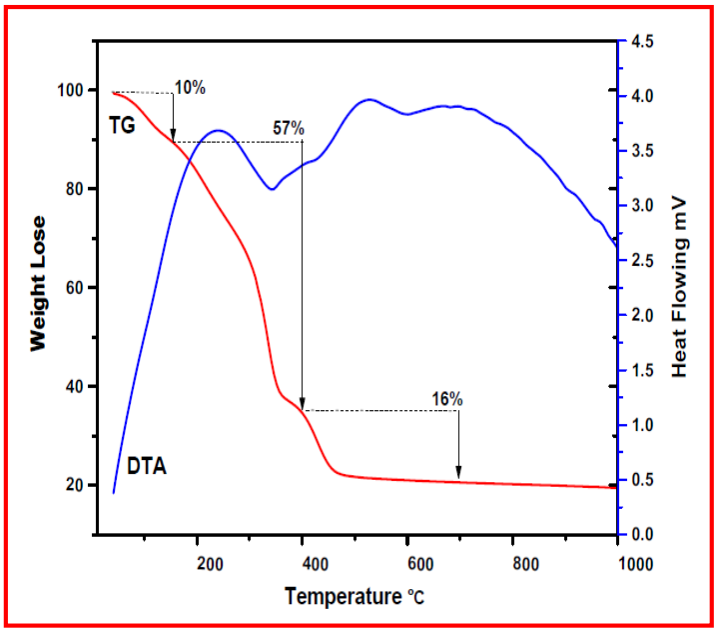

Fig. 2 TG/DTA curve of SiO_2 nanoparticles**.**

3.2. Structural analysis (XRD)

As seen in Fig. 3, the X-ray diffraction patterns verified that the produced SiO_2 samples were amorphous. The broad peak displays a whole amorphous structure. The large peak in the XRD pattern verifies that the produced SiO_2 nanoparticles are amorphous. With the exception of a broad band centered at 22.67°, 22.21°, 21.27° and 20.85° for sample annealed at 500, 600, 700 and 800ºC, respectively. The obtained results indicated that amorphous nature of SiO_2 nanoparticles, there is no diffraction peak. There is no impurity peak for SiO_2 nanoparticles when the findings are compared to the JCPDS file for SiO_2 [4, 20 & 21].

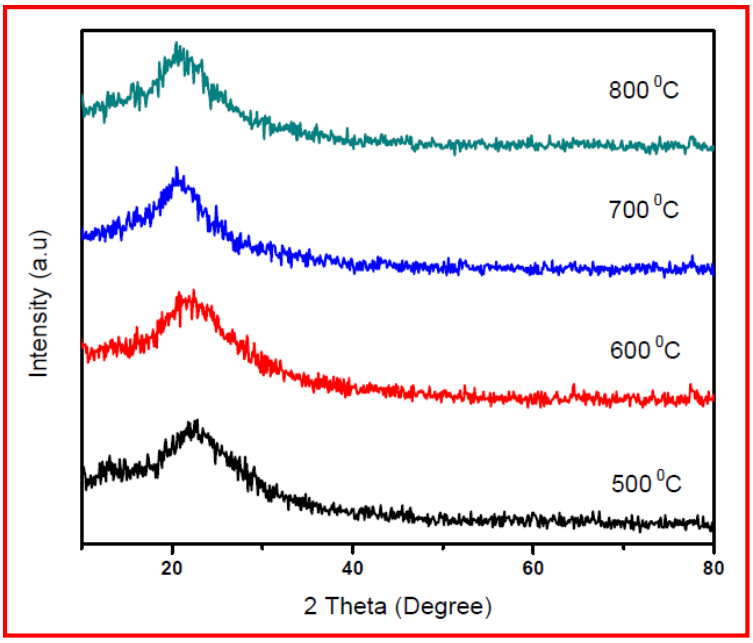

Fig. 3. XRD pattern of SiO_2 nanoparticles with different annealing temperatures.

Using the Scherrer equation, the XRD line broadening data was used to calculate the particles' crystalline size.

$$D = K\lambda / (\beta \cos \theta) \quad (1)$$

Where, λ is the wavelength of CuKα radiation (1.5406 Å), β is full width half maximum (FWHM) of the (hkl) planes, and θ is bragg's diffraction angle by matching the database of the JCPDS file No. 89-1667, the diffraction peaks from Fig. 3 indicate a monoclinic phase structure with a small crystalline size. The average crystalline size of SiO_2 nanoparticles is shown in Table 1.

Table 1. Average Crystallite size of SiO_2 at different annealing temperatures.

S.No	Annealing Temperature (°C)	Average Crystalline Size D (nm)
1	500	61
2	600	59
3	700	42
4	800	34

3.3 Functional group analysis (FT-IR)

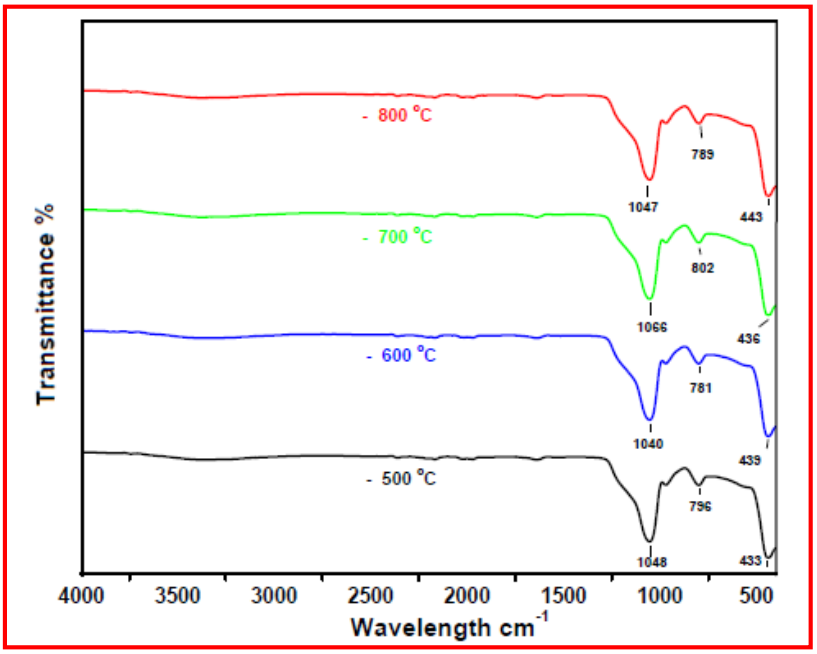

Fig. 4. FT-IR spectrum of SiO_2 nanoparticles at different annealing temperatures.

FT-IR spectra of SiO_2 NPs with various annealing temperatures such as 500 °C, 600 °C, 700 °C and 800 °C were measured wavelength range of 4000 and 400 cm^{-1} are shown in Fig. 4. The presence of O-H stretching bond, which are seen in the region at 1649 to 1669 cm^{-1} [22-24]. The bands, which represents the stretch and asymmetric vibration of Si-O-Si, observed at 1037 to 1065 cm^{-1}. The stretching modes of Si-OH, both symmetric and asymmetric, are responsible for the infrared bands located at 1048 cm^{-1}, 1040 cm^{-1}, 1066 cm^{-1}, and 1047 cm^{-1}. The peak appears at 796 cm^{-1}, 781 cm^{-1}, 802 cm^{-1}, and 789 cm^{-1} is attributed to the stretching and deformation of CH_2 in addition to the hydroxyl groups. Furthermore, the stretching vibration of the metal-oxygen Si-O bond is represented by the transmission band, which has a centre at 433 cm^{-1}, 439 cm^{-1}, 436 cm^{-1}, and 443 cm^{-1} [25 & 26].

3.4 Morphological analysis (SEM-EDX)

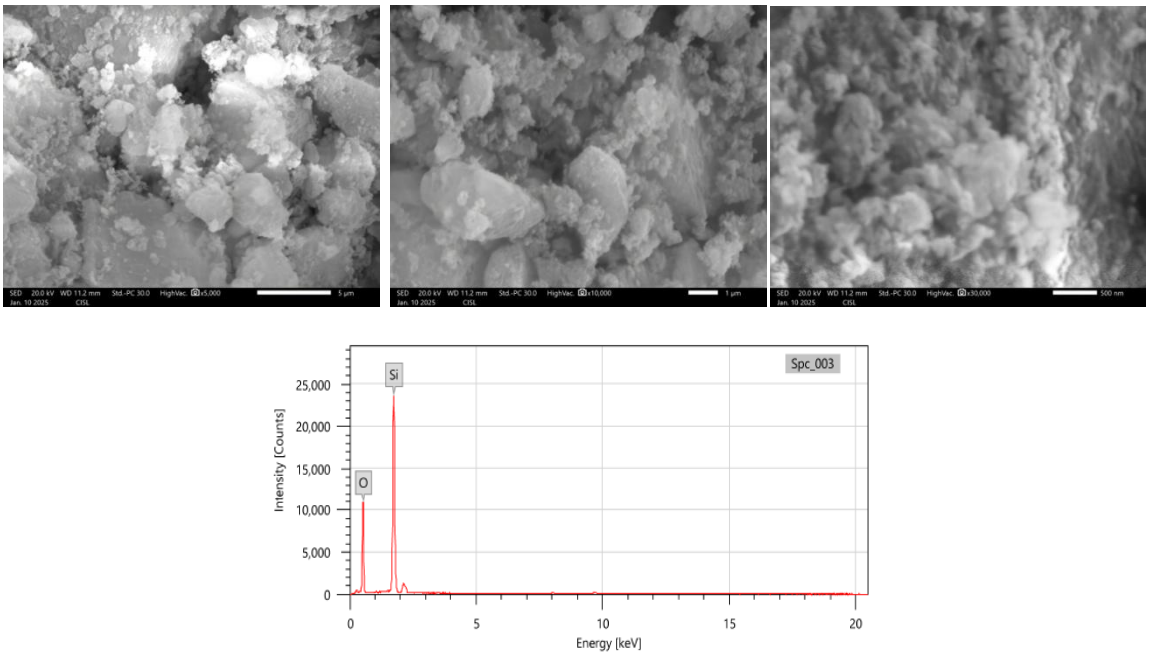

Fig. 5.1. SEM-EDX Micrograph of SiO_2 nanoparticles annealed at 500 °C

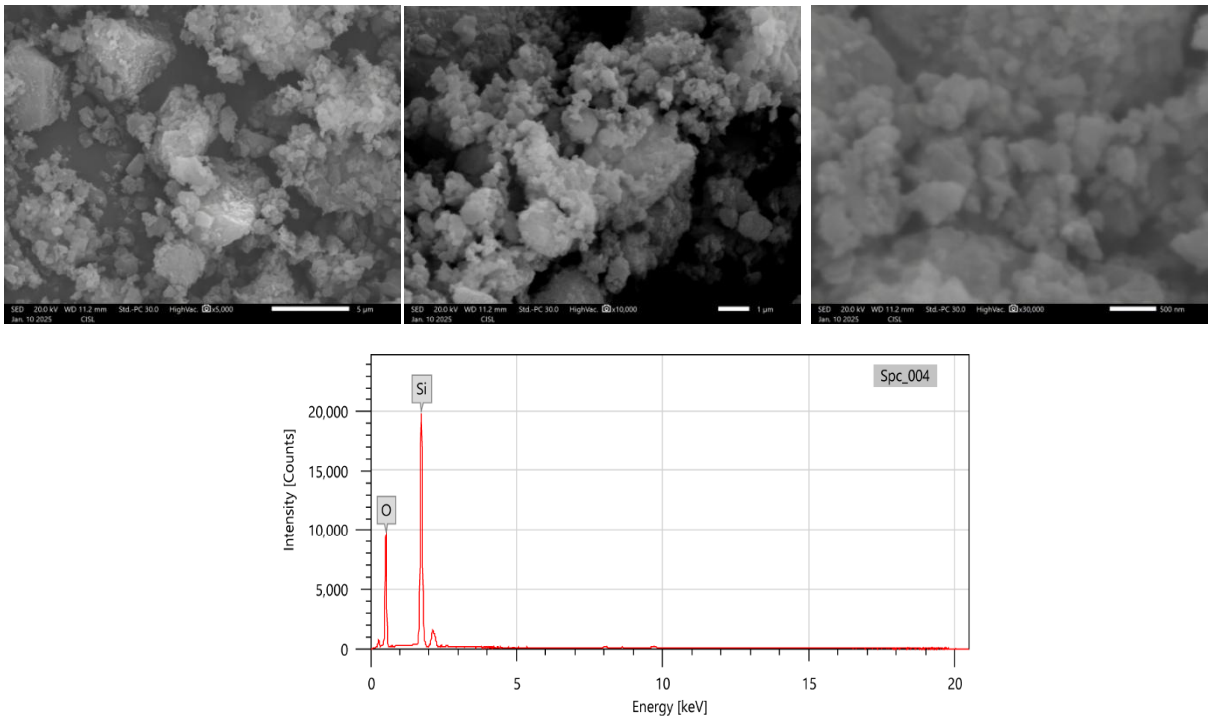

Fig. 5.2. SEM-EDX Micrograph of SiO_2 nanoparticles annealed at 600 °C

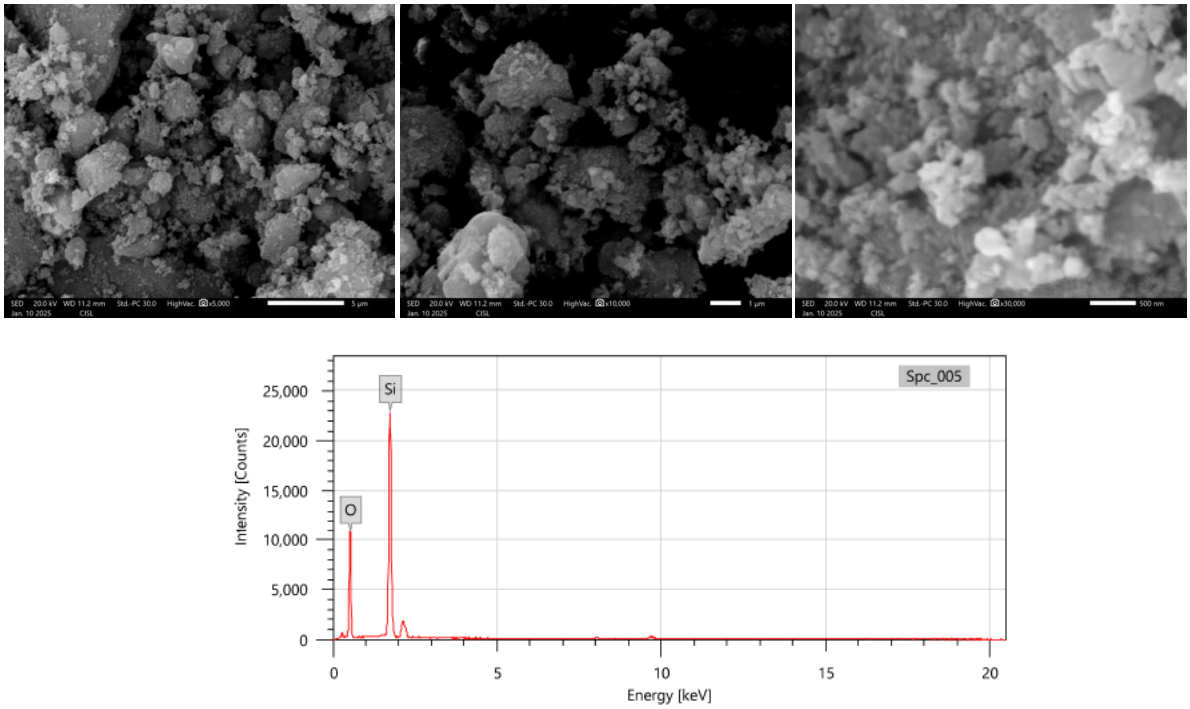

Fig. 5.3. SEM-EDX Micrograph of SiO_2 nanoparticles annealed at 700 °C

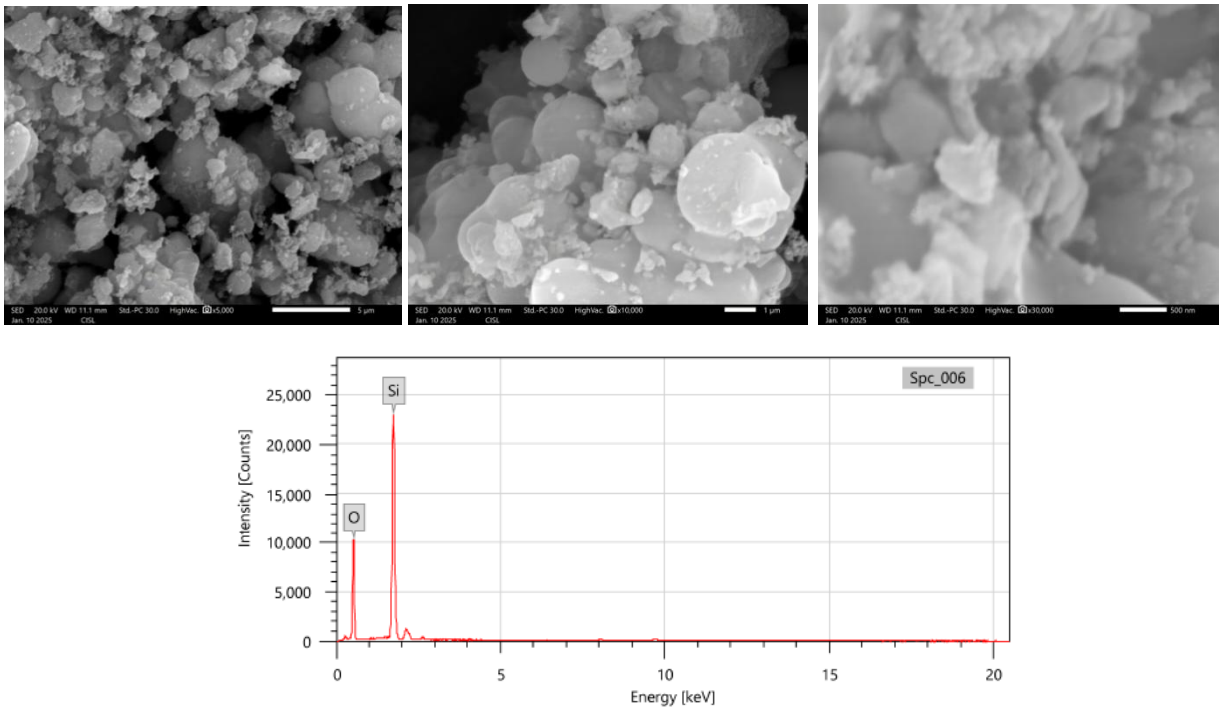

Fig. 5.4. SEM-EDX micrograph of SiO_2 nanoparticles annealed at 800 °C

Through SEM investigation, the SiO_2 nanoparticles morphology was examined. The SiO_2 nanoparticles of SEM micrographs annealed at different temperatures, like 500 °C, 600°C, 700°C and 800°C are displayed in Figs. 5.1 – Figs. 5.4. As observed in the SEM images, the prepared particles are formed aggregated bundle like morphology. According to SEM pictures, the particles range in size from 1µm to 500 nm. Further, increasing the annealing temperature the bundle like morphology changed to spherical particles [27]. A significant number of individual, tiny nanoparticles and agglomerates are present. The EDX spectrum confirmed the presence of elements like Si and O [28 & 29].

3.5 Electrochemical property (CV)

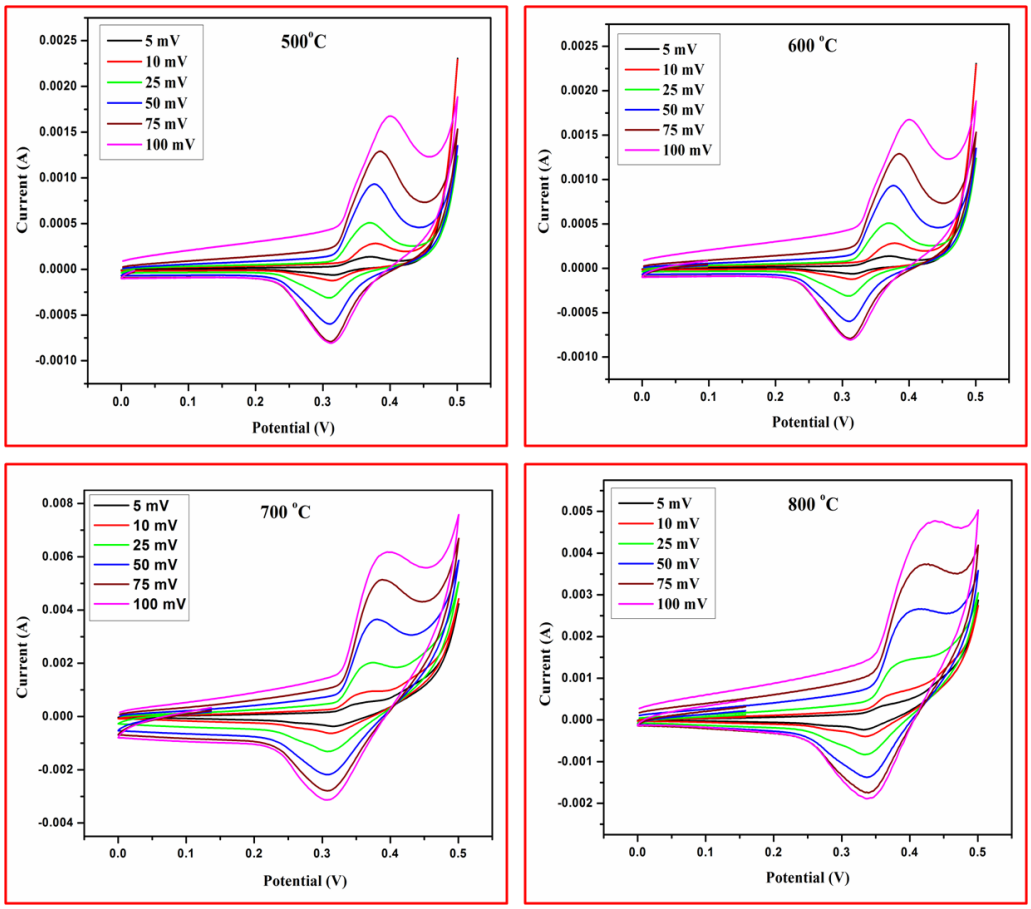

Fig. 6. CV curves of SiO_2 nanoparticles at different scan rates.

The electrochemical property of SiO_2 NPs was studied by using CV analysis. From the CV curves of SiO_2 NPs were recorded at different scan rates (5, 10, 25, 50 and 100 mV/s) in the potential window of -1.5 to +1.5 V and presented in Fig. 6. However, the deviation in the rectangular shape of the curve implies that the sample is having pseudocapacitive nature [30]. From the figure**,** it is observed that for the entire range of scanning, the sample shows the presence of both oxidation and reduction peaks revealing the pseudocapacitive nature of the sample. Such behavior can be described to reversible electrochemical reactions. Additionally, the potential of the anodic and cathodic peaks is seen to shift in less positive and more negative directions, as the scan rate increases [31]. The inability of the ion diffusion rate to adequately counterbalance the electronic naturalization that takes place during the redox process. The specific capacitance (Cs) of the sample can be approximated using the equation [32],

$$Cs = \frac{Q}{\Delta v.m} \qquad (2)$$

Where, Q is the average internal area, Δv is the working Voltage potential range (V) and m is mass of the electrode materials.

The specific capacitance of the synthesized SiO_2 nanoparticles was determined using equation (1), and the results are presented in Table 2. The data indicates that at a scan rate of 5 mVs^{-1}, the samples exhibited peak capacitance values of 310 Fg^{-1}, 325 Fg^{-1}, 356 Fg^{-1}, and 340 Fg^{-1} for the samples annealed at temperatures of 500 °C, 600 °C, 700 °C and 800 °C, respectively. Nevertheless, it is observed that this capacitance value diminishes progressively with an increase in the scan rate. The elevated specific capacitance of SiO_2 suggests its potential applicability in supercapacitor technologies [33-36].

Table. 2 Specific capacitance values of SiO_2 nanoparticles at different scan rates

Scan rate (mV/s)	**Specific capacitance (F/g) 500 °C**	**Specific capacitance (F/g) 600 °C**	**Specific capacitance (F/g) 700 °C**	**Specific capacitance (F/g) 800 °C**
5	310	325	356	340
10	258	261	271	223
25	96	101	129	93
50	54	57	68	51
75	56	53	60	48
100	26	33	36	29

4. Conclusion

The sol-gel approach was effectively used to synthesize and characterize SiO_2 nanoparticles. From the TG-DTA analysis, the endothermic peak at about (240 °C) and exothermic (480 °C) reveals the formation of SiO_2 nanoparticles. A wide peak observed in the XRD spectrum validated the amorphous nature of the synthesized particles, with particle sizes measuring 61 nm, 59 nm, 42 nm, and 34 nm. In FT-IR analysis, clear absorption peaks of were observed, indicating that the nanoparticles were highly hygroscopic in nature. The metal oxygen Si-O bond is represented peak at 433 cm^{-1}, 439 cm^{-1}, 436 $cm^{-1,}$ and 443 cm^{-1}. SEM image of SiO_2 nanoparticles showed the aggregated bundle like morphology. The electrochemical characteristics of SiO_2 nanoparticles have been investigated through cyclic voltammetry. The findings demonstrated specific capacitance values of 310 Fg^{-1}, 325 Fg^{-1}, 356 Fg^{-1}, and 340 Fg^{-1} at a scan rate of 5 mVs^{-1}, indicating their potential use in supercapacitor applications.

References

1. Hongyun Jin , Liang Xu , Shuen Hou, Preparation of spherical silica powder by oxygen-acetylene flame spheroidization process, Journal of Materials Processing Technology, 210, Issue 1, 1 2010, 81-84. https://doi.org/10.1016/j.jmatprotec.2009.08.009.
2. Udayashankar Nithiyanantham , Abdelali Zaki, Yaroslav Grosu , Luis González,Fernández, A. Anagnostopoulos, M.E. Navarro, Y. Ding , Josu Mirena Igartua, Abdessamad Faik, Effect of silica nanoparticle size on the stability and thermophysical properties of molten salts based nanofluids for thermal energy storage applications at concentrated solar power plants., Journal of Energy Storage, 51, July 2022, 104276. https://doi.org/10.1016/j.est.2022.104276.
3. Nayl A. A., A. I. Abd-Elhamid, Ashraf A. Aly and Stefan Bräse., Recent progress in the applications of silica-based nanoparticles, RSC Adv., 2022, 12, 13706–13726. https://doi.org/10.1039/D2RA01587K.
4. Udayashankar Nithiyananthama, Abdelali Zakia, Yaroslav Grosua, Luis González-Fernándeza, Josu M. Igartuab, Abdessamad Faika., SiO_2@Al_2O_3 core-shell nanoparticles based molten salts nanofluids for thermal energy storage applications, Journal of Energy Storage., 26, 2019, 101033. https://doi.org/10.1016/j.est.2019.101033.
5. Sergio Fiorito, Matteo Silvestri, Matilde Cirignano, Andrea Marini, and Francesco Di Stasio, Controlled Growth of Large SiO_2 Shells onto SemiconductorColloidal Nanocrystals: A Pathway Toward Photonic Integration., *ACS Appl. Nano Mater.* 2024, 7, 3724−3733. http://dx.doi.org/10.1021/acsanm.3c05223.
6. Herbert. G., Synthesis of monodispersed silica powders II. Controlled growth reaction and continuous production process, J. Eur. Ceram. Soc. 14, (1994) 205-214. https://doi.org/10.1016/0955-2219(94)90088-4.
7. Vacassy R., R. J. Flatt, Synthesis of Microporous Silica Spheres, J. Colloid and Interface Sci.227 (2000) 302-315. https://doi.org/10.1006/jcis.2000.6860.
8. Nagoo D., H. Osuzu, A. Yamada, E. Mine, Y. Kobayashi, M. Konno, Particle formation in the hydrolysis of tetraethyl orthosilicate in pH buffer solution, J. Colloid Interface Sci. 274, (2004) 143-149. https://doi.org/10.1016/j.jcis.2004.06.041.

9. Vemury S., S.E. Pratsinis, L. Kibbey, Electrically controlled flame synthesis of nanophase TiO_2, SiO_2, and SnO_2 powders, J. Mater. Res. 12, (1997)1031-1042. https://doi.org/10.1557/JMR.1997.0144.
10. Bogush G.H., C. F. Zukoski, Preparation of monodisperse silica particles: Control of size and mass fraction, J. Non. Cryst. Sol. 104, (1988) 95-106. https://doi.org/10.1016/0022-3093(88)90187-1.
11. Kim S.S., H.S. Kim, S.G. Kim, W.S. Kim, Effect of electrolyte additives on sol-precipitated nano silica particles, Ceram. Inte. 30 (2004) 171-175. http://dx.doi.org/10.1016/S0272-8842(03)00085-3.
12. Venkatathri N., Synthesis of mesoporous silica nanosphere using different templates, Sol. Sta.Commun. 143 (2007) 493- 497. http://dx.doi.org/10.1016/j.ssc.2007.06.017.
13. Brinker C. J., G. W. Scherer, Sol-gel Science: the Physics and Chemistry of Sol-gel Processing, Harcourt Brace, San Diego, 1990.
14. Fardad M. A., Catalysts and the structure of SiO_2 sol-gel films, J. Mater. Sci.35 (2000) 1835-1841. https://doi.org/10.1108/JD-01-2016-0005.
15. Prem Ananth, K., Jose, S.P., Nathanael, A.J., Oh, T.H., Mangalaraj, D. and Ballamurugan, A.M., 2016. A Novel Modified sol-gel template Synthesis of high aspect ratio silica nanotubes in the presence of Phosphoric Acid. In Journal of Nano Research (Vol. 35, pp. 27-38). Trans Tech Publications. 10.4028/www.scientific.net/JNanoR.35.27.
16. Corradi, A.B., Bondioli, F., Ferrari, A.M., Focher, B. and Leonelli, C., 2006. Synthesis of silica nanoparticles in a continuous-flow microwave reactor. Powder technology, 167(1), pp.45-48. 10.1016/j.powtec.2006.05.009.
17. Arun Kumar D., Merline Shyla J., Francis P. Xavier., Synthesis and characterization of TiO_2/SiO_2 nano composites for solar cell applications, Applied Nanoscience 2, pp. 429-436, 2012. 10.1007/s13204-012-0060-5.
18. Uda M. N. A., Subash C. B. Gopinath , Uda Hashim , N. H. Halim , N. A.Parmin , M. N. Afnan Uda & Periasamy Anbu., Production and characterization of silica nanoparticles from fly ash: conversion of agrowaste into resource., Preparative Biochemistry & Biotechnology, 2020. http://dx.doi.org/10.1080/10826068.2020.1793174.

19. Blinov A.V., A.A. Blinova, A.A. Kravtsov, A.A. Gvozdenko, A.V. Kobina, E.V. Momot., Synthesis of Multicomponent Systems Based on Silicon Dioxide and Noble Metal Nanoparticles, AIP Conf. Proc. 2188, 040011 (2019). http://dx.doi.org/10.1063/1.5138420
20. Aziz R. A., Sopyan I., Synthesis of TiO_2-SiO_2 powder and thin film photocatalysts of sol-gel method, International Journal of Chemistry 48, 951-957, 2009.
21. Mohan J., Organic spectroscopy principles and applications, 2nd edn. Narosha Publishing House Pvt. Ltd, New Delhi, pp. 28-95, 2009.
22. Saravanan S. and Dubey R.S., synthesis of SiO_2 nanoparticles by sol-gel method and their optical and structural properties ,Romanian journal of information Science and technology volume 23, number 1, 2020, 105–112.
23. Chen, D., Mei, X., Ji, G., Lu, M., Xie, J., Lu, J. and Lee, J.Y., 2012. Reversible Lithium-Ion Storage in Silver-Treated Nanoscale Hollow Porous Silicon Particles. Angewandte Chemie International Edition, 51(10), pp.2409-2413. http://dx.doi.org/10.1002/anie.201107885.
24. Govindhan P., C. Pragathiswaran., Silver Nanoparticle Decorated on ZnO@SiO_2 Nanocomposite and Application for Photocatalytic Dye Degradation of Methylene Blue., Natl. Acad. Sci. Lett.2019. 10.1007/s40009-018-0746-7.
25. Vadim Potapov, Roman Fediuk, Denis Gorev., Obtaining sols, gels and mesoporous nanopowders of hydrothermal nanosilica., Journal of Sol-Gel Science and Technology, 2020. https://link.springer.com/article/10.1007/s10971-020-05216-z.
26. Thu-Huong Le , Dang Thi Thanh Le, and Nguyen Van Tung., Synthesis of Colloidal Silicon Quantum Dot from Rice Husk Ash., Journal of Chemistry Volume 2021, Article ID 6689590, 9 . https://doi.org/10.1155/2021/6689590.
27. Newman, P., Milev, A., Kannangara, K. and Martin, P., 2015. Effect of solvent and silicon substrate surface on the size of iron nanoparticles. Journal of Nanoparticle Research, 17(4), p.164. 10.1007/s11051-015-2963-z.
28. Shokuhfar, A., Eghdam, E. and Alzamani, M., 2012. Effect of Solvent Content on the Properties of Nanostructure Silica Thin Film by Sol-Gel. Nanoscience and Nanotechnology, 2(1), pp.22-25. http://dx.doi.org/10.5923/j.nn.20120201.05.

29. Ramachandran, R., Felix, S., Joshi, G.M., Raghupathy, B.P., Jeong, S.K. and Grace, A.N., 2013. Synthesis of graphene platelets by chemical and electrochemical route. Materials Research Bulletin, 48(10), pp.3834-3842. http://dx.doi.org/10.1016/j.materresbull.2013.05.085.
30. Muhammad Sajjad., Recent Advances in SiO2 Based Composite Electrodes for Supercapacitor Applications, Journal of Inorganic and Organometallic Polymers and Materials, 2021. 10.1007/s10904-021-01899-1.
31. Xuli Ding , Daowei Liang and Hongda Zhao., Enhanced Electrochemical Performance Promoted by Tin in Silica Anode Materials for table and High-Capacity Lithium-Ion Batteries., Materials 2021, 14, 1071. https://doi.org/10.3390/ma14051071.
32. Lavanya Thirugnanam, Dipsikha Ganguly, Ramaprabhu Sundara ., PPy coated on SiO_2 encapsulated porous carbon nanofibers as a potential anode material for high rate capable and long-life Li-ion battery., Materials Letters 298 (2021) 130029. https://doi.org/10.1016/j.matlet.2021.130029.
33. Kevin C. Leonarda, Wendy E. Suyama, Marc A. Anderson, Improvement of electrochemical capacitor electrodes using SiO_2 nanoparticles, Electrochimica Acta 56 (2011) 10137– 10144. https://doi.org/10.1016/j.electacta.2011.08.116.
34. An-YaLo, Chia – Chia Chang, Yi – Wei Lai, Peng – Ren Chen, and Bai – Cheng Xu., Improving the Supercapacitor Performance by Dispersing SiO_2 Microspheres in Electrodes., ACS Omega 2020,5,11522−11528. https://doi.org/10.1021/acsomega.0c00669.
35. YuRong Ren, Bo Yang, HengMaWei, JianNing Ding ., Electrospun SiO_2/C composite fibers as durable anode materials for lithium ion batteries., Solid State Ionics 292 (2016) 27–31. http://dx.doi.org/10.1016/j.ssi.2016.05.002.
36. Yu Yao, Jingjing Zhang, Leigang Xue, Tao Huang, Aishui Yu., Carbon-coated SiO_2 nanoparticles as anode material for lithium ion batteries., Journal of Power Sources 196 (2011) 10240–10243. https://doi.org/10.1016/j.jpowsour.2011.08.009.